# CDOM-DOC relationship in contrasted coastal waters: implication for DOC retrieval from ocean color remote sensing observation.

**Vincent Vantrepotte, [1,2,*] François-Pierre Danhiez,[1] Hubert Loisel, [1,3,4] Sylvain Ouillon,[3,4] Xavier Mériaux,[1] Arnaud Cauvin,[1] and David Dessailly [1,]**

[1] *Laboratoire d'Océanologie et de Géosciences (LOG), Université du Littoral Cote d'Opale, 28 avenue Foch, BP 80, 62930 Wimereux, France*

[2] *CNRS Guyane, USR 3456, 2 av. Charlery, 97300 Cayenne, France*

[3] *Institut de Recherche pour le Développement (IRD), Université de Toulouse, UPS (OMP), UMR 5566 LEGOS, 14 av. Edouard Belin, 31400 Toulouse, France*

[4] *Space Technology Institute (STI), Vietnam Academy of Science & Technology (VAST), 18 Hoang Quoc Viet, Cau Giay, Ha Noi, Vietnam*

[*] *vincent.vantrepotte@univ-littoral.fr*

**Abstract:** Increasing our knowledge on dissolved organic carbon (DOC) spatio-temporal distribution in the coastal ocean represents a crucial challenge for better understanding the role of these ecosystems in the global oceanic carbon cycle. The assessment of DOC concentration from the absorption properties of the colored part of the dissolved organic matter ($a_{cdom}$) was investigated from an extensive data set covering a variety of coastal environments. Our results confirmed that variation in the $a_{cdom}(412)$ to DOC ratio ($a^*_{cdom}(412)$) can be depicted from the CDOM spectral slope in the UV domain ($S_{275\text{-}295}$). They also evidenced that regional first order variation in both $a^*_{cdom}(412)$ and $S_{275\text{-}295}$ are highly correlated to variation in $a_{cdom}(412)$. From these observations, generalized relationships for estimating $a^*_{cdom}(412)$ from $S_{275\text{-}295}$ or $a_{cdom}(412)$ were parameterized from our development sites (N = 158; English Channel, French Guiana, Hai Phong Bay) and tested against an independent data set covering others coastal regions (N = 223; French Polynesia, Rhone River estuary, Gulf of Maine, Chesapeake Bay, Southern Middle Atlantic Bight) demonstrating the possibility to derive DOC estimates from *in situ* CDOM optical properties with an average accuracy of ~16% over very contrasted coastal environments (with DOC ranging from 50 to 250 $\mu mol.L^{-1}$). The applicability of these generalized approaches was evaluated in the context of ocean color remote sensing observation emphasizing the limits of $S_{275\text{-}295}$-based formulations and the potential for $a_{cdom}$-based approaches to represent a compelling alternative for assessing synoptic DOC distribution.



**OCIS codes**: (010.4450) Oceanic optics; (010.1690) Color; (010.1030) Absorption.

## References and links

1. N. R. Bates and D. A. Hansell, "A high resolution study of surface layer hydrographic and biogeochemical properties between Cheasapeake Bay and Bermuda," Mar. Chem. **67**(1-2), 1–16 (1999).
2. J. I. Hedges, "Why dissolved organic matter," in *Biogeochemistry of Marine Dissolved Organic Matter*, D. A. Hansell and C. A. Carlson, ed. (Academic, 2002).
3. W. Ludwig, J. L. Probst, and S. Kempe, "Predicting the oceanic input of organic carbon by continentalerosion," Global Biogeochem. Cycles **10**(1), 23–41 (1996).
4. C. T. A. Chen and A. V. Borges, "Reconciling opposing views on carbon cycling in the coastal ocean: Continental shelves as sinks and near-shore ecosystems as sources of atmospheric $CO_2$," Deep Sea Res. Part II Top. Stud. Oceanogr. **56**(8-10), 578–590 (2009).

#222294 - $15.00 USD Received 3 Sep 2014; revised 9 Nov 2014; accepted 10 Nov 2014; published 5 Jan 2015

5. J. P. Gattuso, M. Frankignoulle, and R. Wollast, "Carbon and carbonate metabolism in coastal aquatic ecosystems," Annu. Rev. Ecol. Syst. **29**(1), 405–434 (1998).
6. C. T. A. Chen, "Exchanges of carbon in the coastal seas," in *The Global Carbon Cycle: Integrating Humans, Climate and the Natural World*, C. B. Field and M. R. Raupach, eds. (Island Press, 2004).
7. V. Borges, B. Delille, and M. Frankignoulle, "Budgeting sinks and sources of CO2 in the coastal ocean: diversity of ecosystems counts," Geophys. Res. Lett. **30**, 1558 (2005).
8. G. M. Ferrari, "The relationship between chromophoric dissolved organic matter and dissolved organic carbon in the European Atlantic coastal area and in the West Mediterranean Sea (Gulf of lions)," Mar. Chem. **70**(4), 339–357 (2000).
9. R. Del Vecchio and N. V. Blough, "Spatial and seasonal distribution of chromophoric dissolved organic matter and dissolved organic carbon in the Middle Atlantic Bight," Mar. Chem. **89**(1-4), 169–187 (2004).
10. N. V. Blough and R. Del Vecchio, "Distribution and dynamics of chromophoric dissolved organic matter (CDOM) in the coastal environment," in *Biogeochemistry of marine dissolved organic matter*, D. A. Hansell and C. A. Carlson, ed. (Academic, 2002).
11. C. Guéguen, L. Guo, and N. Tanaka, "Distribution and characteristics of colored dissolved organic matter in the Western Artic Ocean," Cont. Shelf Res. **25**(10), 1195–1207 (2005).
12. C. E. Del Castillo and R. L. Miller, "On the use of ocean remote sensing to measure the transport of dissolved organic carbon by the Mississippi River Plume," Remote Sens. Environ. **112**(3), 836–844 (2008).
13. A. Mannino, M. E. Russ, and S. B. Hooker, "Algorithm development and validation for satellite-derived distribution of DOC and CDOM in the U.S Middle Atlantic Bight," J. Geophys. Res. **113**(C7), 07051 (2008).
14. C. G. Fichot and R. Benner, "A novel method to estimate DOC concentrations from CDOM absorption coefficients in coastal waters," Geophys. Res. Lett. **38**(3), L03610 (2011).
15. C. G. Fichot and R. Benner, "The spectral slope coefficient of chromophoric dissolved organic matter ($S_{275\text{-}295}$) as a tracer of terrigenous dissolved organic carbon in river-influenced ocean margins," Limnol. Oceanogr. **57**(5), 1453–1466 (2012).
16. R. Lopez, C. E. Del Castillo, R. L. Miller, J. Slisbury, and D. Wisser, "Examining organic carbon transport by the Orinoco River using SeaWiFS imagery," J. Geophys. Res. **117**(G3), G03022 (2012).
17. L. Yang, H. Hong, C. T. A. Chen, W. Guo, and T. H. Huang, "Chromophoric dissolved organic matter in the estuaries of populated and mountainous Taiwan," Mar. Chem. **157**, 12–23 (2013).
18. E. Rochelle-Newall, F. D. Hulot, J. L. Janeau, and A. Merroune, "CDOM fluorescence as a proxy of DOC concentration in natural waters: a comparison of four contrasting tropical systems," Environ. Monit. Assess. **186**(1), 589–596 (2014).
19. J. R. Helms, A. Stubbins, J. D. Ritchie, E. C. Minor, D. J. Kieber, and K. Mopper, "Absorption spectral slopes and slope ratios as indicator of molecular weight, source, and photobleaching of chromophoric dissolved organic matter," Limnol. Oceanogr. **53**(3), 955–969 (2008).
20. C. G. Fichot, K. Kaiser, S. B. Hooker, R. M. W. Amon, M. Babin, S. Bélanger, S. A. Walker, and R. Benner, "Pan-Arctic distributions of continental runoff in the Arctic Ocean," Sci Rep **3**, 1053 (2013).
21. Dessier and J. Donguy, "The sea-surface salinity in the tropical Atlantic between 10°S and 30°N – seasonal and interannual variations (1977 – 1989)," Deep-Sea Res. **1**, 81–100 (1994).
22. V. Vantrepotte, E. Gensac, H. Loisel, A. Gardel, D. Dessailly, and X. Mériaux, "Satellite assessment of the coupling between in water suspended particulate matter and mud banks dynamics over the French Guiana coastal domain," J. S. Am. Earth Sci. **44**, 25–34 (2013).
23. V. Vantrepotte, C. Brunet, X. Mériaux, E. Lécuyer, V. Vellucci, and R. Santer, "Bio-optical properties of coastal waters in the Eastern English Channel," Estuar. Coast. Shelf Sci. **72**(1-2), 201–212 (2007).
24. B. G. Mitchell, M. Kahru, J. Wieland, and M. Stramska, "Determination of spectral absorption coefficients of particles, dissolved material and phytoplankton for discrete water samples," in *Ocean Optics Protocols for Satellite Ocean Color Sensor Validation*, J. L. Mueller, G. D. Fargion and C. R. McClain, eds. (NASA Goddard Space Flight Center, 2003).
25. M. Babin, D. Stramski, G. Ferrari, H. Claustre, A. Bricaud, G. Obolensky, and N. Hoepffner, "Variations in the light absorption coefficients of phytoplankton, non-algal particles, and dissolved organic matter in coastal waters around Europe," J. Geophys. Res. **108**(C7), 3211 (2003).
26. A. Bricaud, A. Morel, and L. Prieur, "Absorption by dissolved organic matter of the sea (yellow substance) in the UV and visible domains," Limnol. Oceanogr. **26**(1), 43–53 (1981).
27. B. Lubac and H. Loisel, "Variability and classification of remote sensing reflectance spectra in the eastern English Channel and southern North Sea," Remote Sens. Environ. **110**(1), 45–58 (2007).
28. X. Pan, A. Mannino, M. E. Russ, and S. B. Hooker, "Remote sensing of the absorption coefficients and chlorophyll *a* concentration in the United States southern Middle Atlantic Bight from SeaWiFS and MODIS-Aqua," J. Geophys. Res. **113**(C11), C11022 (2008).
29. J. Para, P. G. Coble, B. Charrière, M. Tedetti, C. Fontana, and R. Sempéré, "Fluorescence and absorption of chromophoric dissolved organic matter (CDOM) in coastal surface waters of the northwestern Mediterranean Sea, influence of the Rhône River," Biogeosciences **7**(12), 4083–4103 (2010).
30. X. Mari, E. Rochelle-Newall, J. P. Torréton, O. Pringault, A. Jouon, and C. Migon, "Water residence time: A regulatory factor of the DOM to POM transfer efficiency," Limnol. Oceanogr. **52**(2), 808–819 (2007).

#222294 - $15.00 USD Received 3 Sep 2014; revised 9 Nov 2014; accepted 10 Nov 2014; published 5 Jan 2015

31. H. Loisel, X. Mériaux, A. Poteau, L. F. Artigas, B. Lubac, A. Gardel, J. Caillaud, and S. Lesourd, "Analyse of the inherent optical properties of French Guiana coastal waters for remote sensing implications," J. Coastal Res. SI **56**, 1532–1536 (2009).
32. V. Vantrepotte, H. Loisel, D. Dessailly, and X. Mériaux, "Optical classification of contrasted coastal waters," Remote Sens. Environ. **123**, 306–323 (2012).
33. H. Xie, C. Aubry, S. Bélanger, and G. Song, "The dynamics of absorption coefficients of CDOM and particles in the St.Lawrence estuarine system: biogeochimical and physical implications," Mar. Chem. **128-129**(1), 44–56 (2012).
34. L. Bracchini, A. Tognazzi, A. M. Dattilo, F. Decembrini, C. Rossi, and S. A. Loiselle, "Sensitivity analysis of CDOM spectral slope in artificial and natural samples: an application in the central eastern Mediterranean Basin," Aquat. Sci. **72**(4), 485–498 (2010).
35. R. G. M. Spencer, P. J. Hermes, R. Ruf, A. Baker, R. Y. Dyda, A. Stubbins, and J. Six, "Temporal controls of dissolved organic matter and lignin biogeochemistry in a pristine tropical river, Democratic Republic of Congo," J. Geophys. Res. **115**(G3), G03013 (2010).
36. M. A. Granskog, C. A. Stedmon, P. A. Dodd, R. M. W. Amon, A. K. Pavlov, L. de Steur, and E. Hansen, "Characteristics of colored dissolved organic matter (CDOM) in the Artic outflow in the Fram Strait: Assessing the changes and fate of terrigenous CDOM in the Arctic Ocean," J. Geophys. Res. **117**(C12), C12021 (2012).
37. R. G. M. Spencer, K. D. Butler, and G. R. Aiken, "Dissolved organic carbon and chromophoric dissolved organic matter properties of river in the USA," J. Geophys. Res. **117**(G3), G03001 (2012).
38. E. Ortega-Retuerta, T. K. Frazer, C. M. Duarte, S. Ruiz-Halpern, A. Tovar-Sánchez, J. M. Arrieta, and I. Reche, "Biogeneration of chromophoric dissolved organic matter by bacteria end krill in the Southern Ocean," Limnol. Oceanogr. **54**(6), 1941–1950 (2009).
39. C. L. Osburn and C. A. Stedmon, "Linking the chemical and optical properties of dissolved organic matter in the Baltic-North Sea transition zone to differentiate three allochtonous inputs," Mar. Chem. **126**(1–4), 281–294 (2011).
40. E. J. D'Sa, "Colored dissolved organic matter in coastal waters influenced by the Atchafalaya River, USA: Effects of an algal bloom," J. Appl. Remote Sens. **2**(1), 023502 (2008).
41. A. Matsuoka, S. B. Hooker, A. Bricaud, B. Gentili, and M. Babin, "Estimating absorption coefficients of colored dissolved organic matter (CDOM) using a semi-analytical algorithm for southern Beaufort Sea waters: application to deriving concentrations of dissolved organic carbon from space," Biogeosciences **10**(2), 917–927 (2013).
42. Q. Dong, S. Shang, and Z. Lee, "An algorithm to retrieve absorption coefficient of chromophoric dissolved organic matter from ocean color," Remote Sens. Environ. **128**, 259–267 (2013).
43. H. Loisel, V. Vantrepotte, D. Dessailly, and X. Mériaux, "Assessment of the colored dissolved organic matter in coastal waters from ocean color remote sensing," Opt. Express **22**(11), 13109–13124 (2014).
44. C. G. Fichot, S. E. Lohrenz, and R. Benner, "Pulsed, cross-shelf export of terrigenous dissolved organic carbon to the Gulf of Mexico," J. Geophys. Res. **119**(2), 1176–1194 (2014).
45. C. Goyens, C. Jamet, and T. Schroeder, "Evaluation of four atmospheric correction algorithms for MODIS-AQUA image over contrasted coastal waters," Remote Sens. Environ. **131**, 63–75 (2013).

## 1. Introduction

Dissolved organic carbon (DOC) represents the largest reservoir of organic carbon in the ocean [1–4]. Considering the large DOC inputs from terrestrial ecosystems and marine production as well as the important fluxes occurring in coastal waters through carbon mineralization or export processes, the understanding of DOC dynamics in continental margins represents a key issue for better constraining the actual role of these ecosystems in the global carbon cycling [5–7]. This however represents an important challenge considering the wide spatial and temporal variability of DOC loads in these ecosystems where numerous and complex physical and biogeochemical factors regulate the interaction between the diverse source or sink processes controlling this carbon reservoir.

The understanding of the actual carbon stock represented by ocean margins DOC and its fate over the river to ocean continuum is currently limited by the very few information available on DOC distribution in these waters, with data often restricted to very punctual observations. The crucial need of an increasing spatial and temporal coverage in DOC measurements can be however facilitated by the possible assessment of DOC distribution from *in situ* or satellite measurements of the optical properties (absorption, fluorescence) of the colored part of the dissolved organic matter (CDOM). The use of CDOM optical properties as a proxy for DOC concentration relies however on an accurate characterization of the CDOM-DOC relationship. The presence of significant linear CDOM-DOC relationships have been documented in various estuarine and coastal domains in the recent years [8–18].

#222294 - $15.00 USD Received 3 Sep 2014; revised 9 Nov 2014; accepted 10 Nov 2014; published 5 Jan 2015

While the latter studies have evidenced that CDOM and DOC behave consistently in coastal waters dominated by terrestrial discharges due to the conservative mixing of CDOM and DOC along the salinity gradient, they also illustrated the wide variability existing in the linkage between CDOM and DOC at both seasonal and regional scales. This feature can be attributed to temporal modulations as well as to spatial heterogeneity in DOC and CDOM inputs and removing processes. In addition to variability in catchment area characteristics and estuarine biogeochemical processes [15–17], variation in the importance of photodegradation processes affecting differently CDOM and DOC kinetics or modulations in the relative contribution of the autochthonous production of DOM have been shown to be major factors modifying or altering the connection between CDOM and DOC [13, 14].

Recently, Helms et al. [19] have documented that the CDOM slope in the UV domain (275-295 nm, $S_{275-295}$) represents a relevant indicator of DOM molecular weight which variation indicates DOM origin and photochemical history. These latter characteristics of $S_{275-295}$ make this parameter to represent a valuable proxy for assessing the natural variability of the DOC specific absorption coefficient ($a^*_{cdom}(\lambda) = a_{cdom}(\lambda)/DOC$). This capability was recently confirmed by Fichot and Benner [14,15] who clearly demonstrated that $S_{275-295}$ represents an excellent tracer of the relative contribution of the terrigenous organic carbon (tDOC) in river dominated coastal domains. Specifically, the connection between $S_{275-295}$ and $a^*_{CDOM}(\lambda)$ in river influenced coastal sites, has been related to the dual nature of lignin being an important chromophore in CDOM and a terrigenous component of DOC in riverine influenced systems [14,17]. Besides, the effects of physical mixing and photodegradation processes on $S_{275-295}$ have been shown to be the major forcing parameters shaping the non-linear relationship between the two latter parameters [15]. Information on CDOM spectral slope coefficient in the UV domain therefore appears to represent a valuable information for deriving basin scale DOC estimates as recently illustrated from a pan-arctic application based on satellite remote sensing information [20].

The present study aims at characterizing the link between CDOM absorption properties and DOC content within three contrasted coastal ecosystems under the influence of terrestrial inputs of DOM (Eastern English Channel, French Guiana, and Vietnam). The specific aims are to define $a_{cdom}$-DOC relationships in these three coastal sites and to test the pertinence of $S_{275-295}$ for describing variation in the $a_{cdom}$/DOC ratio when considering regional heterogeneities in DOM origin and dynamics. The practical use of this proxy for improving our ability to assess DOC in the context of large scale ocean color remote sensing application is finally specifically assessed from the data gathered in the latter three coastal sites as well as from independent CDOM-DOC data set gathering a variety of coastal waters differently impacted by DOM terrestrial discharges. A simple approach to derive the CDOM spectral slope coefficient in the UV domain is proposed in this context.

#222294 - $15.00 USD Received 3 Sep 2014; revised 9 Nov 2014; accepted 10 Nov 2014; published 5 Jan 2015

## 2. Materials and methods

### *2.1. Development data set*

#### 2.1.1 Sampling strategy

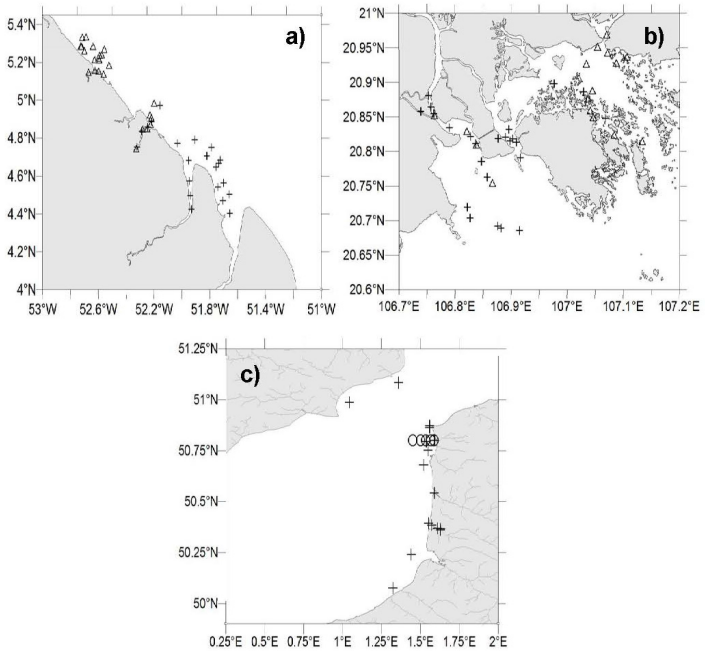


Fig. 1. Location of the stations sampled in the frame of this study. (a) French Guyana cruises in 2010 (triangle) and 2012 (cross). (b) VITEL cruises sampling stations within the Hai Phong bay and Red River Delta in Vietnam in 2011 (triangle) and 2013 (cross).(c) Stations biweekly visited along a coastal-offshore transect (circle) in the eastern English Channel or during short episodic cruises within coastal and estuarine waters of the English Channel (cross) in 2012 and 2013.

Three contrasted coastal sites were investigated in both estuarine and marine waters (N = 158) for the development of the model (Table 1, Fig. 1). These three coastal sites allow a wide representation of the natural variation in DOC and CDOM dynamics in both temperate and tropical waters with watershed differently influenced by anthropogenic forcing. About 77% of the stations are directly impacted by river inputs, while the others (N = 36) are under oceanic influence. The present data set only gathers measurements performed in the sea surface layer (< 2 m).

The first site is the French Guiana coastal waters sampled during dry (October 2010, N = 24) and wet seasons (May 28 to June 05 2012, N = 25, Fig. 1(a)) with stations specifically located in water masses influenced by the Oyapock, Approuague, Mahury and Kourou rivers. In addition to the impact of these local rivers, this tropical coastal domain is characterized by permanent influence of the Amazon River outputs [21,22]. The second site corresponds to the Vietnamese coastal water masses located in Red River Delta, Ha Long and Hai Phong Bays sampled during the dry season (November 2011, N = 17) and the wet season (June 2013, N = 24) (Fig. 1(b)). The last site is the coastal zone of the eastern English Channel, and in the Authie and Canche rivers, which has been sampled during winter and early spring season in 2012 and 2013 (N = 68, Fig. 1(c)). This coastal area is influenced by rivers of lesser importance (e.g. Somme and Seine rivers) when compared to the two previous ones, being also characterized by the presence of a strong phytoplankton spring bloom which potentially modulates the regional DOM dynamics in this area [23].

#222294 - $15.00 USD Received 3 Sep 2014; revised 9 Nov 2014; accepted 10 Nov 2014; published 5 Jan 2015

**Table 1. Description of the development and validation (in bold) data sets.**

| Site | Date | Number of stations |
|---|---|---|
| French Guiana | 17 - 21 October 2010 | 24 |
| | 28 May - 05 June 2012 | 25 |
| Vietnam | 07 - 17 November 2011 | 17 |
| | 28 June – 07 July 2013 | 24 |
| Eastern English Channel | 03 February-19 April 2012 | 43 |
| | 28 February – 04 April 2013 | 25 |
| **French Polynesia** | 22 – 29 November 2004 | 32 |
| **Rhone River** | December 2007 – April 2009 | 17 |
| **SeaBASS** (Southern Middle Atlantic Bight) | BIOME 1: 30 March – 1 April 20005 | 20 |
| | BIOME 2: 26 –30 July 2005 | 19 |
| | BIOME 3: 9 –12 May 2006 | 50 |
| **SeaBASS** (Cheasapeake Bay) | 5 May 2005 | 9 |
| | 3 November 2005 | 13 |
| | 6 September 2007 | 17 |
| **SeaBASS** (Gulf of Maine) | BIOD01: 26 – 30 April 2007 | 15 |
| | BIOD02: 26 – 28 May 2007 | 18 |
| | BIOD03: 6 – 8 June 2007 | 13 |

### 2.1.2 CDOM absorption

CDOM absorption spectra were measured following the NASA protocol [24]. Seawater samples were filtered under gentle vacuum (<5 mm Hg) through 0.2 µm polycarbonate membranes (Whatman Nuclepore, 47 mm). Samples were placed in pre-combusted (450°C, 6h) brown glass bottles and stored under refrigeration (4°C) until laboratory analysis. Before the analysis, CDOM samples were reheated to room temperature to avoid any bias induced by temperature differences between sample and reference (Milli-Q water). CDOM absorbance spectra were measured every nanometer from 250 to 850 nm using a double-beam Ultraviolet-Visible spectrophotometer (Shimadzu, UV-2450) with a 100 mm Suprasil quartz cell. CDOM absorption coefficient ($a_{cdom}(\lambda)$) are then calculated from absorbance measurements using the following equation:

$$a_{cdom}(\lambda) = 2.303.A(\lambda) / L \quad (1)$$

where A(λ) is the absorbance of the filtered seawater sample at the specific wavelength λ and L is the optical pathway of the quartz cell in meters (here 0.1 m).

As recommended by Babin et al [25] a baseline correction was applied to each spectrum by subtracting the average absorbance in the range 680-690 nm to the whole spectrum. The absorption spectral shape of CDOM is typically described through a single exponential function [26]:

$$a_{cdom}(\lambda) = a_{cdom}(\lambda_0)e^{-S(\lambda-\lambda_0)} \quad (2)$$

where $a_g(\lambda)$ is the absorption coefficient at the wavelength λ, $a_{cdom}(\lambda_0)$ the absorption coefficient at reference wavelength $\lambda_0$, and S the spectral slope in the spectral range from $\lambda_0$ to λ with $\lambda_0 < \lambda$.

Variation in the spectral signature of CDOM in the UV domain has been shown to be appropriated for investigating DOC/CDOM relationship in various coastal sites [14,19]. In

#222294 - $15.00 USD Received 3 Sep 2014; revised 9 Nov 2014; accepted 10 Nov 2014; published 5 Jan 2015

this study, $S_{cdom}$ was therefore derived between 275 and 295 nm ($S_{275-295}$) through a log-linearization of CDOM absorption spectra.

2.1.3. DOC concentration

Glass bottles and vials used for filtering and storing DOC samples were previously cleaned (basic detergent sodium hydroxide, Extran® MA 01, and 10% diluted HCl solution), then rinsed with ultrapure water (resistivity ≥ 18.2 MΩ.cm$^{-1}$, ultraviolet oxidized) and finally placed at 450°C for 6 hours. Seawater samples for DOC analysis were filtered under gentle vacuum (< 5 mm Hg) through 0.7 µm pre-combusted 47 mm glass fiber membranes (Whatman GF/F). For each station, DOC was sampled in triplicate and stored under refrigeration (4°C) before analysis for short storage duration time (<24 h). For longer storage periods, samples were acidified (0.1% hydrochloric acid) prior to refrigeration in order to minimize DOC biological alteration processes.

DOC concentrations (µmol.L$^{-1}$) were measured by High Temperature Combustion Oxidation (HTCO, Shimadzu TOC-VCSH). 100 $\mu$L injections of every sample were repeated (three to five times) until the coefficient of variation of the measurements decreased below 2%. The accuracy of [DOC] measurements was checked at device startup and then every six samples using the deep sea water consensus reference material (CRM, Hansell Laboratory, Rosenstiel School of Marine and Atmospheric Science, University of Miami) from batch 12, 2012 (41-44 µmol.L$^{-1}$). Calibration curves were computed using potassium hydrogen phthalate solution (KHP) ranging from 10 to 400 µmol.L$^{-1}$. A new calibration curve was performed after each catalyst and air bottle replacement. The instrument carbon blank was obtained by averaging numerous ultrapure water injections (N = 90, mean = 4.78 µmol.L$^{-1}$). This value (4.78 µmol.L$^{-1}$) was then subtracted from each sample measurement and only samples with an absolute difference under 10% between triplicates were considered.

2.1.4 Ancillary data

In addition to the latter discrete samples in CDOM and DOC, vertical profiles of salinity, temperature were acquired with a Sea Bird Electronics SBE37-SI probe. For Guianese and Vietnamese samples only, the marine reflectance was acquired with TRIOS radiometers according to the protocol described in Lubac and Loisel [27].

*2.2 Validation data set*

Besides the samples collected in the three coastal sites investigated, a validation data set was built gathering external sea surface (depth < 4m) CDOM and DOC measurements. This data set is firstly composed by measurements hosted by the SeaBass database (NASA Ocean Biology Processing Group, seabass.gsfc.nasa.gov). The latter data have been collected during multiple cruises conducted within the coastal waters of the southern Middle Atlantic Bight between 2005 and 2007 (N = 39, BIOD01, BIOD02, BIOD03), Chesapeake Bay (N = 89, BIOME1, BIOME2, BIOME3) and Gulf of Maine (N = 46, BIODIVERSITY) [13,28]. Further, data from the Rhône river delta (France, N = 19 [29],), and from a tropical lagoon (southwest lagoon of New Caledonia, N = 32 [30],) were also considered. This validation data set therefore covers a wide range of biogeochemical conditions. Waters of the southern Middle Atlantic Bight are strongly impacted by riverine discharge into the Delaware and Chesapeake Bays, and are characterized by large variability range for $a_{cdom}(412)$ ([0.05 –1 m$^{-1}$]) and [DOC] ([50 – 250 µmol.L$^{-1}$]) values. Data from the Rhône river delta are strongly under the influence of freshwater inputs with high levels of $a_{cdom}(412)$ ([0.5 – 1.5 m$^{-1}$]) and [DOC] ([67 – 216 µmol.L$^{-1}$]). Data from the southwest lagoon of New Caledonia consists in shallow water samples (< 20 m depth) characterized by terrestrial inputs from the nearshore domain into surrounding ultra-oligotrophic oceanic waters and therefore presents the lowest range of $a_{cdom}(412)$ ([0.03 – 0.41 m$^{-1}$]) and [DOC] ([59 – 85 µmol.L$^{-1}$]) values.

#222294 - $15.00 USD Received 3 Sep 2014; revised 9 Nov 2014; accepted 10 Nov 2014; published 5 Jan 2015

*2.3 Statistics*

The accuracy of [DOC], $a^*_{cdom}$ (412) and $S_{275\text{-}295}$ estimates has been evaluated using various statistical indicators including the root mean squared difference (RMSD), the mean relative absolute difference (MRAD) and the mean relative difference (Bias) expressed respectively as:

$$RMSD = \sqrt{\frac{\sum_{i=1}^{N}(y_i - x_i)^2}{N}} \quad (3)$$

$$MRAD = 100.\frac{1}{N}\sum_{i=1}^{N}\frac{|y_i - x_i|}{x_i} \quad (4)$$

$$Bias = 100.\frac{1}{N}\sum_{i=1}^{N}\frac{y_i - x_i}{x_i} \quad (5)$$

where N is the number of samples in the data set, $x_i$ the measured value and $y_i$ the estimated value of the parameter of interest.

## 3. Results and discussion

*3.1 CDOM optical properties and DOC content variability*

Samples collected in Vietnam and French Guiana coastal regions globally illustrate the range of variability between freshwaters and marine end-members (salinity [0 ; 34.8 psu] and [0 ; 32 psu], respectively) while measurements performed in the estuarine and coastal waters of the eastern English Channel are mostly representative of brackish and marine waters with salinity values higher than 18 psu (Table 2). The overall range of variation in $a_{cdom}(412)$ and DOC for the whole data set is [0.097-4.054 $m^{-1}$] and [51-253 µmol.$L^{-1}$], respectively. The maximal $a_{cdom}(412)$ and DOC values are observed in Guianese estuarine waters reflecting the larger riverine inputs of DOM for these tropical coastal waters [31, 32]. Vietnamese samples show in comparison lower $a_{cdom}(412)$ and DOC values for low salinity extreme samples (0.78 $m^{-1}$ and 174 µmol.$L^{-1}$). Data for the eastern English Channel correspond to coastal water masses influenced by river discharges of lesser amplitude and are in agreement with the range of variation already reported for this coastal region [8, 23, 25].

**Table 2. Median, standard deviation, and range values of salinity, $a_{cdom}(412)$, $S_{275\text{-}295}$, DOC, $a^*_{cdom}(412)$ measurements in the French Guiana, eastern English Channel and Vietnamese coastal waters.**

| | French Guiana | Eastern English Channel | Vietnam |
|---|---|---|---|
| Salinity | 25.55 ; 11.17<br>[0.02 –34.82]<br>(N = 49) | 34.2 ; 2.88<br>[18.4 – 35.24]<br>(N = 68) | 21.33 ; 11.42<br>[0.27 – 31.95]<br>(N = 41) |
| $a_{cdom}(412)$ | 0.63 ; 0.96<br>[0.097 – 4.054]<br>(N = 49) | 0.19 ; 0.07<br>[0.128 – 0.506]<br>(N = 68) | 0.38 ; 0.20<br>[0.14 – 0.791]<br>(N = 41) |
| $S_{275\text{-}295}$ | 0.0145 ; 0.0015<br>[0.0116 –0.018]<br>(N = 25) | 0.0231 ; 0.002<br>[0.0154 – 0.0258]<br>(N = 68) | 0.0182 ; 0.0023<br>[0.0155 – 0.0256]<br>(N = 41) |
| [DOC] | 113.88 ; 38.47<br>[83.18 – 253.38]<br>(N = 49) | 78.97 ; 17.66<br>[51.0 ± 158.18]<br>(N = 68) | 108.99 ; 24.73<br>[75.48 – 174.32]<br>(N = 41) |
| $a^*_{cdom}(412)$ | 0.0057 ; 0.00407<br>[0.00094 –0.01995]<br>(N = 49) | 0.0025 ; 0.00044<br>[0.00168 –0.00373]<br>(N = 68) | 0.0032 ; 0.00107<br>[0.00144 –0.00601]<br>(N = 41) |

Salinity in psu, $a_{cdom}(412)$ in $m^{-1}$, $S_{275\text{-}295}$ in $nm^{-1}$, DOC in µmol.$L^{-1}$, $a^*_{cdom}(412)$ in $m^2$.$mmol^{-1}$, N represents the number of samples.

#222294 - $15.00 USD Received 3 Sep 2014; revised 9 Nov 2014; accepted 10 Nov 2014; published 5 Jan 2015

For each site, strong negative relationships are found between $a_{cdom}(412)$, DOC and salinity ($p<0.001$, Figs. 2(a) and 2(b)). These CDOM and DOC dilution gradients from fresh to marine waters underline the predominant impact of terrestrial inputs in the dynamics of DOM for the coastal sites investigated. Besides this general pattern, the dispersion found for each site in the CDOM or DOC dependence with salinity reflects variation in DOM sources and mixing processes experienced during the different cruises performed within these coastal margins. As a matter of fact, the large dispersion around the linear mixing curve for the low salinity waters of French Guiana (S < 25 psu, Figs. 2(a) and 2(b)) reveals the multiple riverine sources of DOM as well as seasonal modulation between wet and dry seasons. Similarly, the high scatter observed in the eastern English Channel especially for the most marine DOC samples (S > 32 psu) might be related to the seasonal variation in the relative contribution of marine produced DOM in these waters [23].

The $a_{cdom}(412)$/DOC ratio (thereafter denoted as $a^*_{cdom}(412)$) values range from 0.00094 to 0.01995 $m^2.mmol^{-1}$ from marine dominated to freshwater dominated environments (Table 2). $a^*_{cdom}(412)$ salinity gradient however present strong regional variation in the removal and mixing processes affecting DOC and CDOM in the different coastal margins investigated. As a matter of fact, the decreasing gradient in $a^*_{cdom}(412)$ with salinity was particularly strong in French Guiana with $a^*_{cdom}(412)$ values diminishing by a factor of 21.2 from fresh to oceanic waters. This pattern contrasts with the smoother dilution patterns observed in the Vietnamese and eastern English Channel waters where $a^*_{cdom}(412)$ decreased by a factor of 4.2 and 2.2 along the salinity gradient, respectively. These regional heterogeneities were particularly marked for samples with salinity <32 psu (Fig. 2(c)) while $a^*_{cdom}(412)$ inter or intra-site variability in the marine domain (S > 32 psu) was very weak with data slightly varying around an average value of 0.0024 $m^2.mmol^{-1}$ (overall CV = 21%).

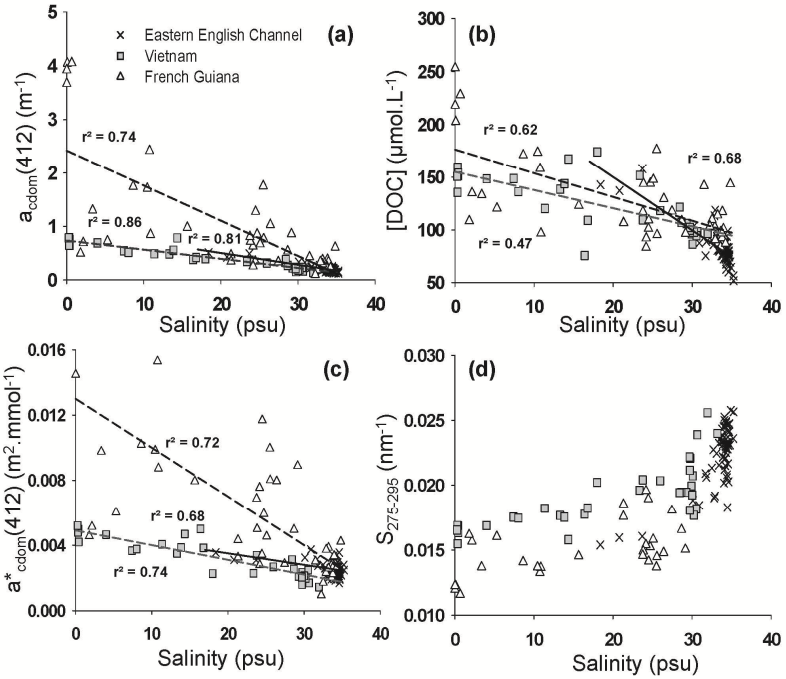


Fig. 2. Relationships between salinity and a) $a_{cdom}(412)$, b) DOC, c) $a^*_{cdom}(412)$ and d) $S_{275-295}$, for the French Guiana, Vietnam and eastern English Channel coastal waters.

A strong nonlinear dependence between $S_{275-295}$ and salinity was observed within the three coastal sites investigated (Fig. 2(d)). While the lowest $S_{275-295}$ values were observed in

#222294 - $15.00 USD Received 3 Sep 2014; revised 9 Nov 2014; accepted 10 Nov 2014; published 5 Jan 2015

freshwaters environments (minimum of 0.0112 $nm^{-1}$ in French Guiana), $S_{275-295}$ increased sharply towards marine waters reaching a maximum value of 0.0258 $nm^{-1}$ in the eastern English Channel (Table 2). The latter spatial patterns for the CDOM spectral signature in the UV domain were not associated with concurrent trends in the visible part of the spectrum (not shown) in agreement with previous observations performed in various coastal environments [15, 17, 19, 33–35]. Such variation in $S_{275-295}$ along the salinity gradient underlines the potential for this optical descriptor to be used as a relevant tracer of the terrestrial origin of the dissolved organic matter. Specifically, increasing patterns in $S_{275-295}$ are related to the decrease in the molecular weight and aromaticity of CDOM from fresh to marine waters [19, 36, 37]. Fichot and Benner [15] demonstrated from a detailed study based on *in situ* and experimental measurements that this non linear pattern does not correspond to a simple dilution process but is rather shaped by the joint impact of the physical mixing of chromophores of fresh and marine origin and an increased influence of photobleaching processes along the salinity (turbidity) gradient. Conversely, other processes such as flocculation, biological activity (microbial alteration or marine production of DOM), variations in the water masses characteristics (e.g. pH, ionic strength or inorganic species: nitrate, nitrite) or inputs from re-suspension processes have been shown to have only a moderated or restricted impact on $S_{275-295}$ natural variability [15–19].

### *3.2 Regional CDOM-DOC relationships*

The overall co-variation in the dilution patterns for CDOM and DOC allows the definition of significant linear regional relationships between the latter two parameters (Fig. 3). While these parameterizations should be confirmed from extended *in situ* sampling allowing to fully capture the whole salinity gradient as well as seasonal variation in DOM origin, our results suggest the potential for CDOM absorption coefficient to be used as a valuable proxy from estimating DOC in the three coastal sites investigated from *in situ* or remote sensing $a_{cdom}(412)$ observations. This confirms the observations already documented by several authors in a variety of continental margins influenced by terrestrial inputs of DOM [8–14, 16, 17].

Strong regional discrepancies are however observed between the three coastal sites investigated (Figs. 3(a)-3(c)). Slope values of the $a_{cdom}(412)$ vs DOC relationship in the eastern English Channel (213.3 $(\mu mol.L^{-1}).m^{-1}$) and Vietnamese coastal waters (94.13 $(\mu mol.L^{-1}).m^{-1}$) are in the range of those documented in other coastal areas (e.g [13]. and references therein). Conversely, the slope for the French Guiana coastal waters significantly departs from the two latter regions (32.9 $(\mu mol.L^{-1}).m^{-1}$ at 412 nm) being at the lower end of the values already reported for estuarine environments (e.g [17, 35].). The latter features are coherent with the high average CDOM specific absorption coefficient $a^*_{cdom}(412)$ for this area (0.01535 $m^2.mmol^{-1}$) when compared to the two other coastal sites (0.00556 and 0.01043 $m^2.mmol^{-1}$ for the English Channel and Vietnamese coastal waters, respectively). Similar features are observed for the intercept which is maximal in French Guiana emphasizing a low proportion of uncolored DOC (95.6 $\mu mol.L^{-1}$) while this proportion tends to increase in the coastal waters of Vietnam and in the eastern English Channel (80.8 $\mu mol.L^{-1}$ and 38.0 $\mu mol.L^{-1}$, respectively). The latter regional variations in the coefficients of the CDOM-DOC relationships are related to modulations in DOM origin as well as in the regulating processes acting on its dynamics. The impossible generalization of such $a_{cdom}$ to DOC relationships for deriving synoptic DOC estimates in coastal waters is also illustrated from the large discrepancies between the parameterizations derived from our data set and those already reported in other coastal regions at 355 nm (Fig. 3(d) [9, 13, 18],).

#222294 - $15.00 USD Received 3 Sep 2014; revised 9 Nov 2014; accepted 10 Nov 2014; published 5 Jan 2015

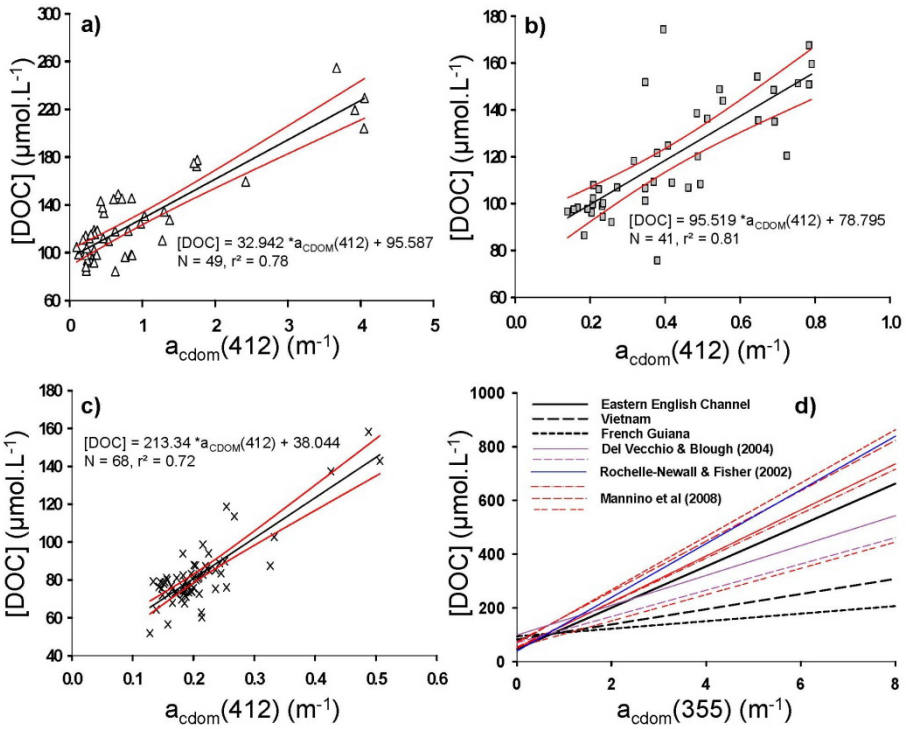


Fig. 3. $a_{cdom}(412)$-DOC linear relationships (black lines) in (a) French Guiana, (b) Vietnamese coastal waters, and (c) the eastern English Channel. The red lines in (a), (b), and (c) delimit the 95% confidence intervals. The relationships at 355 nm in these three regions (eastern English Channel: N = 68, $r^2$ = 0.77, Vietnam: N = 41, $r^2$ = 0.73, French Guiana: N = 49, $r^2$ = 0.79) are compared with those reported in the literature for diverse coastal waters under the influence of river discharges in DOM (Middle Atlantic Bight (MAB), Chesapeake Bay (CB) and Delaware Bay (DB) [9, 13, 18].

### *3.3 Generalized parameterizations*

#### 3.3.1 $S_{275\text{-}295}$ based approach

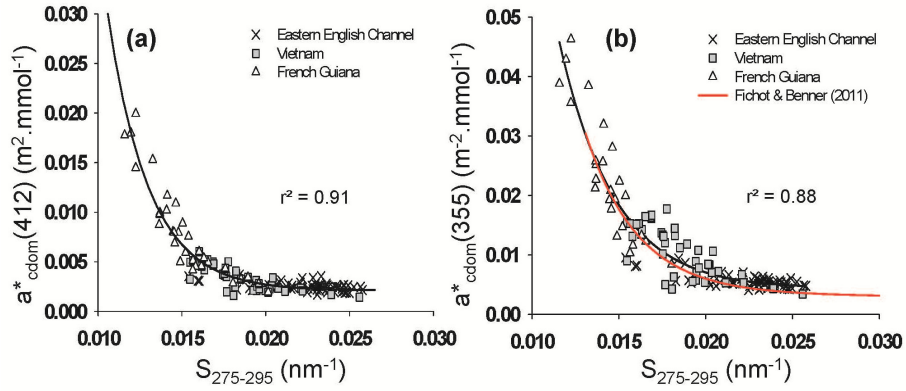


Fig. 4. a) Relationship between $a^*_{cdom}(412)$ and $S_{275\text{-}295}$ for the development data set gathering data collected in French Guiana, Vietnamese and English Channel coastal waters. The same relationship is provided at 355 nm (b) for comparison with Fichot and Benner [14].

#222294 - $15.00 USD Received 3 Sep 2014; revised 9 Nov 2014; accepted 10 Nov 2014; published 5 Jan 2015

Variations in $S_{275\text{-}295}$ are associated with opposite trend patterns in $a^*_{cdom}(412)$ (Fig. 4). High $S_{275\text{-}295}$ are associated with low DOC-normalized absorption in marine samples while low $S_{275\text{-}295}$ correspond to high DOC-normalized absorption in estuarine or freshwater environments (Fig. 4). The capability of $S_{275\text{-}295}$ to be used as tracer of the natural variations in $a^*_{cdom}(412)$ [19] is further confirmed by the presence of strong relationships $S_{275\text{-}295}$-$a_{cdom}(412)$/DOC ratio for each site investigated ($p<0.001$). More interestingly, this tight relationships between $a^*_{cdom}(412)$ and $S_{275\text{-}295}$ presents a conservative pattern when samples for the three sites are gathered together (Fig. 4(a)), leading to a unique formulation such as:

$$a^*_{cdom}(412) = a.(e^{(b.S_{275-295})} - e^{(c.S_{275-295})}) + d \quad (6)$$

where a = 12.47; b = –553, c = 0.01097 and d = 12.48 ($p<0.001$, N = 158) This relationship confirms that the same processes (i.e physical mixing and photodegradation) regulate these two optical properties of DOM in river influenced coastal margins [15, 19, 38]. This feature has been in particularly associated with the importance in these coastal environments of lignin content being at the time an important chromophore driving CDOM optical properties and a major component of terrestrial DOC [15]. Our results confirm that $S_{275\text{-}295}$ can be used as a valuable proxy for better constraining scatter around CDOM-DOC relationship and therefore improving estimates of DOC content from DOM optical properties [14, 15, 17, 19, 35, 39]. This study further suggests the potential for $S_{275\text{-}295}$ to represent a relevant indicator of the DOC-normalized absorption coefficient for large scale applications in riverine influenced coastal margins. This capability is underlined by relatively low scatter and site to site variations around the general $S_{275\text{-}295}$-$a^*_{cdom}(412)$ relationship when compared to the sharp heterogeneity observed in the direct $a_{cdom}(412)$-DOC relationships (Fig. 3). The previous statement is further confirmed by the general consistency between the parameterization defined from the three coastal sites investigated in the frame of this study and the ones recently reported in other works [14, 15, 20] performed in distinct coastal regions (i.e. Mississippi river plume, Arctic waters) although differences in the ranges of observation (Fig. 4(b)). Note that the data points collected out of the influence of river inputs do not depart from the proposed relationships, underlying the potential application of Eq. (6) for a large range of coastal waters (at least in the condition of a weak contribution of autochthonous DOM production, as discussed below).

Further, in the condition of a predominant impact of riverine discharge on DOM variability a significant relationships can be drawn between $a_{cdom}(412)$ and $S_{275\text{-}295}$ (Fig. 5). Interestingly, while this connection is observed in the three coastal sites investigated taken individually, it is remarkable to observe that it remains valid when all the data are pulled together conducting to a unique parameterization ($p<0.001$, N = 158) such as:

$$S_{275-295} = \frac{(0.0425 + 0.1061.a_{cdom}(412))}{1 + 9.238.a_{cdom}(412)} \quad (7)$$

As previously observed for the $S_{275\text{-}295}$-$a^*_{cdom}(412)$ relationship, Eq. (7) also stands for the data points far from rivers influence. The use of such a general formulation allows for $S_{275\text{-}295}$ to be retrieved with an average accuracy of ± 5.4%, with 86.6% of the data presenting a relative error < 10% (Fig. 5). This therefore suggests that site to site variation in $S_{275\text{-}295}$ can be primarily associated with the relative importance of $a_{cdom}(412)$ which can be related in the three sites investigated to that of the terrestrial inputs in DOM. Further, this also indicates that the relative impact of the regulatory processes acting on CDOM optical properties behave conservatively among these three river dominated coastal margins.

#222294 - $15.00 USD Received 3 Sep 2014; revised 9 Nov 2014; accepted 10 Nov 2014; published 5 Jan 2015

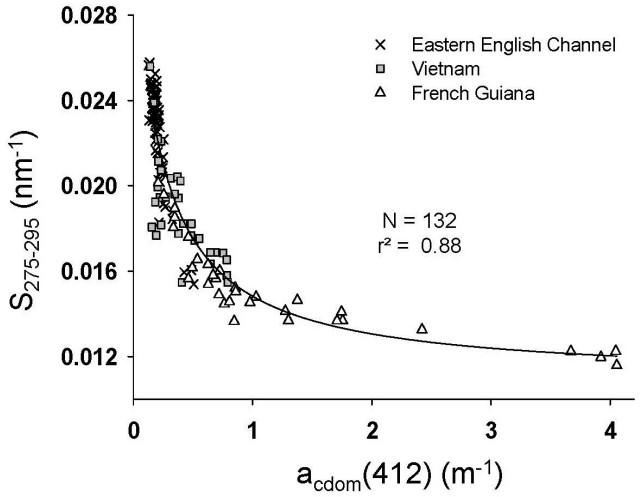


Fig. 5. Relationship between $a_{cdom}(412)$ and $S_{275-295}$ obtained for the development data set.

The combination of the formalisms in Eqs. (6) and (7) might therefore represents a valuable alternative for better constraining variations in $a^*_{cdom}(412)$ and ultimately synoptically derive DOC concentration from ocean color observation specifically in coastal environment where DOM dynamics is principally affected by continental inputs. Note however, that the present results should be confirmed over a wider range of $S_{275-295}$ covering especially higher $S_{275-295}$ values ([0.025-0.5 $nm^{-1}$] more representative of coastal waters with relative low CDOM and DOC loads ([15, 20] and references therein).

3.3.2 $a_{cdom}(412)$ based approach

The significance of Eqs. (6) and (7) considering multisite data eventually tends to suggest that while direct relationships between $a_{cdom}(412)$ and DOC cannot be generalized among various coastal domains, first order variation in the CDOM specific absorption coefficient can be related to the relative importance of terrestrial inputs which can be approximated, in the assumption of river dominated coastal systems, by variation in $a_{cdom}(412)$. This is illustrated in Fig. 6 by the highly significant relationship between $a_{cdom}(412)$ and $a^*_{cdom}(412)$ which can be expressed as follows:

$$a^*_{cdom}(412) = 10^{(0.7109.\log_{10}(a_{cdom}(412))-2.1722)} \quad (8)$$

#222294 - $15.00 USD Received 3 Sep 2014; revised 9 Nov 2014; accepted 10 Nov 2014; published 5 Jan 2015

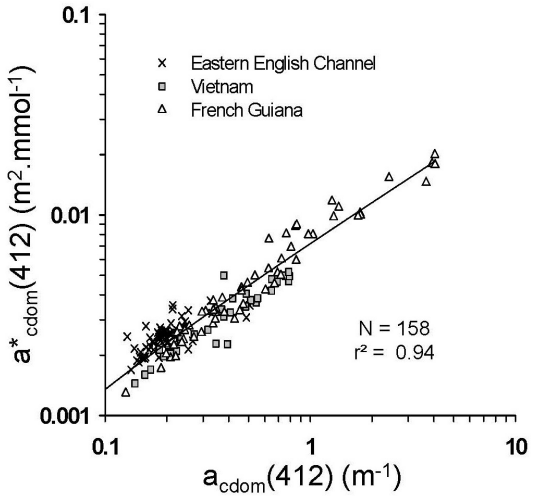


Fig. 6. Relationship between $a_{cdom}(412)$ and $a^*_{cdom}(412)$ in the three geographical areas investigated.

This result therefore emphasizes that while the direct computation of DOC from $a_{cdom}(412)$ is conceivable at a regional scale only (Fig. 3(d)), information held by $a_{cdom}(412)$ is however exploitable to depict site to site variation in $a^*_{cdom}(412)$ thus representing a possible alternative for deriving large scale DOC estimates.

3.3.3 Relative performance of regional and generalized approaches

The relative accuracy of DOC retrieval from region specific (Fig. 3) and broader relationships has been compared on the data gathered in eastern English Channel, French Guiana, and Vietnamese waters (Figs. 7 and 8, Table 3). This cannot be considered as a validation exercise (as the same data set is used for the development and the evaluation), but rather to an evaluation of the actual impact of generalized approaches on DOC retrieval. Statistics for the three costal sites indicate $a^*_{cdom}(412)$ can be estimated with a comparable accuracy from $S_{275-295}$ (Eqs. (6) and (7)) or directly from $a_{cdom}(412)$ (Eq. (8)) with a RMSD, MRAD and Bias of 0.0007 and 0.0008 ($m^2$ . $mmol^{-1}$), 13 and 14% and 3 and 5%, respectively (N = 158, Fig. 7).

Logically, similar patterns are found for the corresponding DOC statistics with RMSE, MRAD and bias of 17 and 18 µmol.$L^{-1}$, 14 and 15% and 5 and −8% for the two approaches, respectively. Although these general statistics indicate an expected decrease in DOC retrieval accuracy using generalized approaches when compared to region-specific $a_{cdom}(412)$-DOC linear relationships (RMSD = 16 µmol.$L^{-1}$, MRAD = 9% and Bias = 1%, Fig. 8), the detailed values at regional scale (Table 3) indicate that the largest loss in precision induced by a generalization of the DOC inversion algorithm is observed for the poorly DOC loaded marine waters of the eastern English Channel where variation in $a^*_{cdom}(412)$ was found to be particularly weak (Fig. 4). The latter general statistics however provide encouraging evidence of the possible assessment of DOC content from $a_{cdom}(412)$ over large spatial scale in coastal waters.

#222294 - $15.00 USD Received 3 Sep 2014; revised 9 Nov 2014; accepted 10 Nov 2014; published 5 Jan 2015

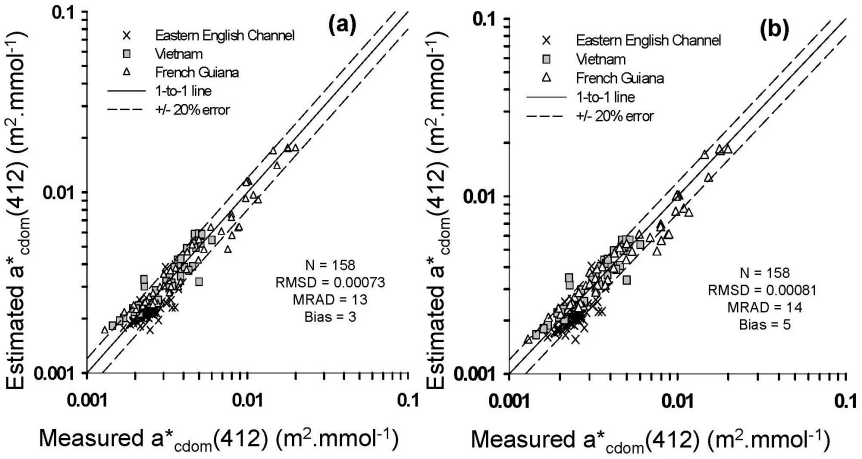


Fig. 7. Scatter plots of the retrieved $a^*_{cdom}(412)$ values using (a) the general formulations in Eqs. (6) and (7) ($S_{275\text{-}295}$ based method) and (b) Eq. (8) ($a_{cdom}(412)$ based method) as a function of the measured $a^*_{cdom}(412)$ values for the development data set. The solid lines represent 1:1 line and the dashed lines represents the 20% error lines.

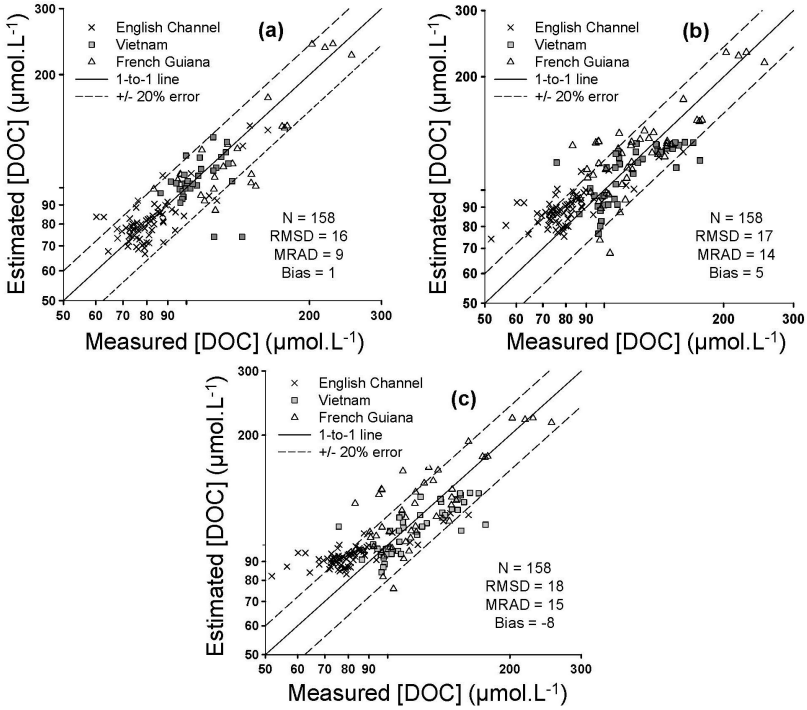


Fig. 8. Scatter plots of the DOC retrieved values from (a) regional $a_{cdom}(412)$-DOC relationships (b) the $S_{275\text{-}295}$ based method, and (c) the $a_{cdom}(412)$ based method, as a function of the measured DOC values. The solid lines represent the 1:1 line, and the dashed lines represents the 20% error lines. The values of statistical indicators are provided in each panel.

#222294 - $15.00 USD Received 3 Sep 2014; revised 9 Nov 2014; accepted 10 Nov 2014; published 5 Jan 2015

**Table 3. Statistics for $a^*_{cdom}(412)$ and DOC retrievals using the regional $a_{cdom}(412)$ vs DOC relationships derived for each site investigated and the two proposed generalized formulations.**

| | | Regional[a] | $S_{275-295}$ based method[b] | | $a_{cdom}$ based method[c] | |
|---|---|---|---|---|---|---|
| | | [DOC] | $a^*_{cdom}(412)$ | [DOC] | $a^*_{cdom}(412)$ | [DOC] |
| French Guiana | RMSD | 16 | 0.0011 | 20 | 0.0012 | 21 |
| | MRAD | 11 | 13 | 14 | 13 | 15 |
| | Bias | 1 | 1 | –4 | 3 | –6 |
| | N | 49 | 49 | 49 | 49 | 49 |
| Eastern English Channel | RMSD | 9 | 0.00041 | 13 | 0.00048 | 16 |
| | MRAD | 8.81 | 12.07 | 14 | 16 | 19 |
| | Bias | 1 | 9 | –12 | 13 | –16 |
| | N | 68 | 68 | 68 | 68 | 68 |
| Vietnam | RMSD | 16 | 0.00005 | 16 | 0.0005 | 17 |
| | MRAD | 9 | 12 | 12 | 11 | 10 |
| | Bias | 0 | –6 | 4 | –6 | 4 |
| | N | 41 | 41 | 41 | 41 | 41 |

[a]Fig. 3., [b]using Eqs. (6) and (7), [c]using Eq. (8), N indicates the total number of samples, $a^*_{cdom}(412)$ is expressed in $m^2.mmol^{-1}$ and DOC in $\mu mol.L^{-1}$.

The pertinence of the proposed generalized parameterizations has been further tested against an independent data set gathering samples from contrasted coastal waters (N = 225) not necessarily dominated by river inputs. The resulting estimates of $a^*_{cdom}(412)$ and DOC are represented in Fig. 9 and Table 4. On average, $a^*_{cdom}(412)$ and DOC are restituted with a relative accuracy of 15 and 16% for the $S_{275-295}$ based approach and 15 and 13% considering the $a_{cdom}(412)$ based approach, respectively. While, the latter results should be complemented by an extended data set covering specifically coastal margins with low DOM conditions, we note that the performance of the proposed generalized formulations globally stand for $a^*_{cdom}(412) < 0.002$ $m^2.mmol^{-1}$ and DOC <70 $\mu mol.L^{-1}$. The largest departure from the 1:1 line for both $a^*_{cdom}(412)$ and DOC are associated with samples presenting relatively high Chlorophyll *a* loads, individuated as data for which [Chl*a*] (when available) was greater than the last quartile computed for each cruise individually (Fig. 9). In this context of high Chl*a* loads, representing conditions potentially associated with a significant contribution of marine produced DOM, $a^*_{cdom}(412)$ is largely overestimated conducting to a strong underestimation of the DOC content (Fig. 9). When discarding these samples, the percentage of data presenting an absolute relative error in DOC retrieval greater than 20% decreases from 26 to 10%. This certainly underlines the limit of validity of the proposed general approaches which performance is restricted to water masses where DOM inputs are mostly of riverine and terrestrial (land washing, re-suspended sediment, etc) origin. This also further emphasizes the need to better characterize the impact of phytoplankton degradation on DOM optical properties and carbon content dynamics in these highly productive ecosystems. This apparent limitation might be however explicitly considered through the use of optical classification approaches allowing the definition of the range of applicability of the latter methods on a pixel basis [32].

#222294 - $15.00 USD Received 3 Sep 2014; revised 9 Nov 2014; accepted 10 Nov 2014; published 5 Jan 2015

**Table 4. Statistics for $a^*_{cdom}(412)$ and DOC retrievals for the validation data set using the two proposed generalized formulations.**

| | | $S_{275\text{-}295}$ based method[a] | | $a_{cdom}$ based method[b] | |
|---|---|---|---|---|---|
| | | $a^*_{cdom}(412)$ | [DOC] | $a^*_{cdom}(412)$ | [DOC] |
| French Polynesia | RMSD | 0.0004 | 12 | 0.00041 | 13.62 |
| | MRAD | 12 | 14 | 12 | 15 |
| | Bias | 4 | –6 | 8 | –11 |
| | N | 32 | 32 | 32 | 32 |
| Rhône River | RMSD | 0.00119 | 12 | 0.00048 | 21 |
| | MRAD | 30 | 14 | 16 | 13 |
| | Bias | 11 | –6 | 13 | 3 |
| | N | 17 | 17 | 17 | 17 |
| SeaBASS | RMSD | 0.0005 | 21 | 0.0005 | 23 |
| | MRAD | 14 | 12 | 11 | 13 |
| | Bias | –9 | 6 | –6 | 4 |
| | N | 174 | 174 | 174 | 174 |

[a]Using Eqs. (6) and (7), [b]using Eq. (8), N indicates the total number of samples, $a^*_{cdom}(412)$ is expressed in $m^2.mmol^{-1}$ and DOC in $\mu mol.L^{-1}$.

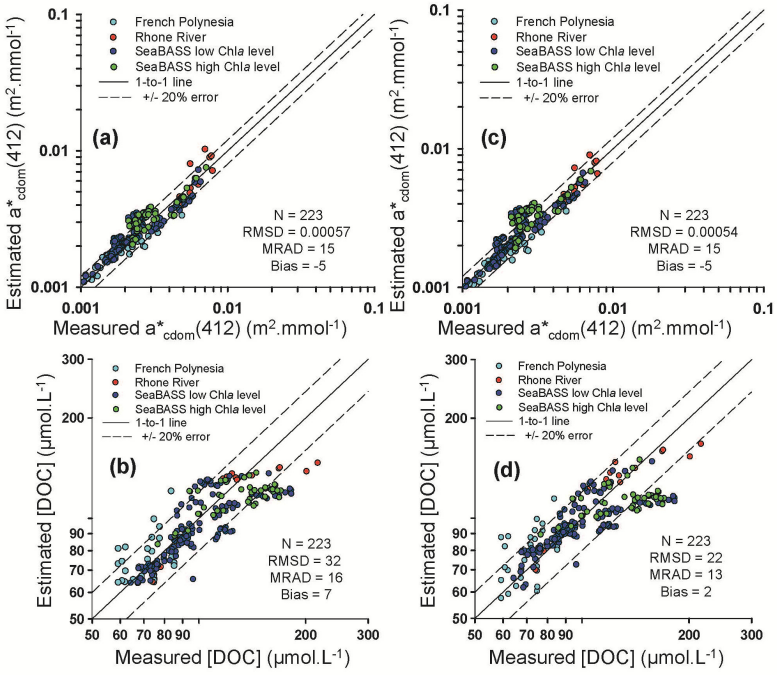


Fig. 9. $a^*_{cdom}(412)$ and DOC retrieved from the general formulations in Eqs. (6) and (7) ($S_{275\text{-}295}$ based method, a), b)) and in Eq. (8) ($a_{cdom}(412)$ based method c), d) for the validation data set. Samples represented in green correspond to data with relatively high levels of Chl*a* (see text). The solid lines represent the 1:1 line, and the dashed lines represents the 20% error lines.

#222294 - $15.00 USD Received 3 Sep 2014; revised 9 Nov 2014; accepted 10 Nov 2014; published 5 Jan 2015

The previous results developed on three contrasted coastal sites and validated over five coastal regions covering a wide range of CDOM ($S_{275\text{-}295}$, $a^*_{cdom}(412)$) and DOC ([50-250 $\mu mol.L^{-1}$]) properties emphasize the potential of such unified $S_{275\text{-}295}$ or $a_{cdom}(412)$ based approaches for deriving DOC content over coastal margins where DOM dynamics is principally driven by terrestrial forcing. The interest of the latter methods precisely stands in their applicability over a large panel of coastal environments (e.g. from estuarine to tropical lagoon) thus providing encouraging evidence on the possibility to derive DOC estimates over very contrasted coastal waters. This seems conversely to be hardly achievable in practice through the use of regional approach which would imply the development of a mosaic of site specific algorithms.

Further, while our results tend to indicate that simple linear CDOM-DOC relationships should be preferred for studying DOC dynamics over a specific region, it should be pointed that the large seasonal variation in the $a_{cdom}$ vs DOC dependence, already reported in diverse coastal sites [e.g 13,20.] and probably not fully represented from the data sets gathered in the three development sites, might represent a real practical issue in the application of such straightforward methods. This also re-enforces the interest of using proxies such as those proposed in the two unified approaches for better constraining region specific variations in $a^*_{cdom}(412)$ (as already documented for $S_{275\text{-}295}$ [20,44]).

### *3.4 Implication for remote sensing applications*

A key issue for deriving DOC estimates from remote sensing observation first relies on an accurate estimation of CDOM absorption properties. The specific assessment of $a_{cdom}$ from the marine reflectance is complicated by the optical similarity of CDOM and non-algal particles which make them very difficult to distinguish from ocean color observation. This represents a major issue in coastal waters where the relative contribution of these two optically significant components of seawater to the overall non-water absorption can drastically change at both regional and temporal scales [23, 25, 32]. In the recent years, diverse empirical (e.g [13, 40].) or semi analytical algorithms (e.g [41–43].) have been developed to face this issue now allowing to derive $a_{cdom}(\lambda)$ in coastal waters from remote sensing observation with a satisfying accuracy.

Our results have further confirmed the interest of estimating $S_{275\text{-}295}$ for better constraining the variability in $a^*_{cdom}(412)$ values. A challenge for deriving synoptic estimates of DOC from satellite observation, thus also concerns our ability to depict the information held by the CDOM spectral signature in the UV domain from ocean colour data. A possible approach for mapping $S_{275\text{-}295}$ has been proposed in Eq. (6) based on $a_{cdom}(412)$ distribution. Another alternative proposed by Fichot et al. [20] has been recently illustrated from a pan-arctic study showing that $S_{275\text{-}295}$ can be estimated directly from remote sensing information using a multi-linear parameterization of the MODIS marine reflectance (i.e. $R_{rs}$ at 443, 488, 531, 555 and 667 nm). This $R_{rs}$ based alternative has been shown to provide $S_{275\text{-}295}$ estimates with a similar accuracy than using Eq. (6) ( ± 4%). This possibility to derive basin scale maps of $S_{275\text{-}295}$ from spatial remote sensing information has been further validated (for $S_{275\text{-}295}$ ranging from 0.02 to 0.05 $m^{-1}$) from a similar study dedicated to the coastal waters of the Gulf of Mexico [44] based on a different combination of MODIS $R_{rs}$ bands (i.e. at 443, 488, 555 667 and 678 nm).

The possible generalization of the approach has been tested against Vietnamese and French Guiana data for which concurrent CDOM and marine reflectance measurements have been performed. The application of the algorithms by Fichot et al [20,44] on our data set shows varying performance (Fig. 10) in its potential to retrieve $S_{275\text{-}295}$ emphasizing that such algorithms might be un-adapted for certain coastal areas or should be regionally tuned for being fully exploitable. This underlines the probable inadequacy of such reflectance-based approach for deriving synoptic $S_{275\text{-}295}$ estimates in coastal waters. The overall scatter in Fig. 10 can be related to the fact that the link between marine reflectance in the visible and CDOM

#222294 - $15.00 USD Received 3 Sep 2014; revised 9 Nov 2014; accepted 10 Nov 2014; published 5 Jan 2015

spectral signature in the UV is not fully related to concurrent changes in the CDOM spectral slope between these two optical domains as illustrated by previous studies ([15] and references therein) and confirmed from our results. A significant link between $R_{rs}$ and $S_{275\text{-}295}$ mostly rely (i) on the presence of a predominant impact of CDOM on the water optical budget, as observed in arctic waters [41], and (ii) on a significant co-variation between CDOM and particulate matter dynamics (i.e. phytoplanktonic, mineral and detrital particles). The latter conditions are apparently not verified in both Vietnamese and French Guiana coastal waters in agreement with the strong spatio-temporal heterogeneity in the relative contribution of dissolved and particulate matter to the water masses optical characteristics for these two coastal margins [31, 32]. Further, in the context of remote sensing application, the use of such multi-linear formulation for estimating $S_{275\text{-}295}$ presents the clear disadvantage to be highly sensible to the cumulated uncertainties associated with the reflectance signal at the different bands considered. As a matter of fact, considering the relative percentage differences computed in coastal waters between estimated and calculated reflectance values for the MODIS visible bands [45], the use of Fichot et al. formalism [20] would for instance conduct to an average analytical error of −8.6% in $S_{275\text{-}295}$ reaching up to −60% in $S_{275\text{-}295}$ in high sediment loaded environments. Reporting these uncertainties in Eq. (6) would lead to an over-estimation in DOC of about 38% and 98%, respectively.

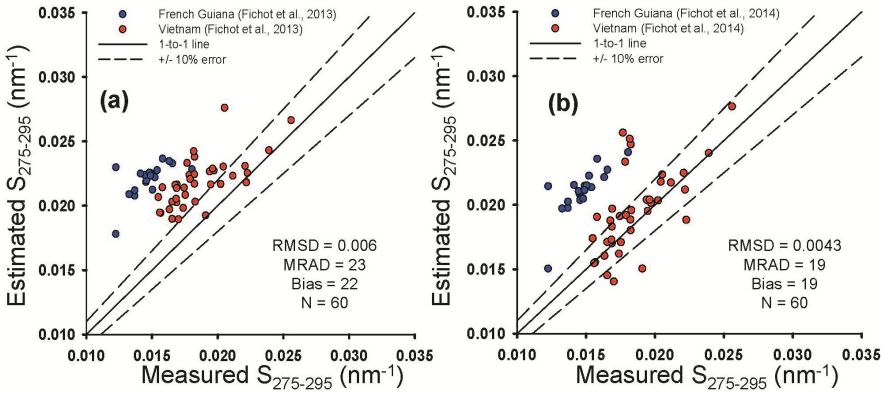


Fig. 10. $S_{275\text{-}295}$ retrieval obtained from a multi-linear combination of the MODIS marine reflectance using the original algorithms by Fichot et al. [20] and Fichot et al. [44] applied to the Vietnamese and French Guiana samples.

The performance of the two unified approaches presented in the frame of this study for deriving DOC from ocean color remote sensing are highly related to the uncertainties in $a_{cdom}(412)$ values. This impact has been evaluated considering various levels of $a_{cdom}(412)$ (i.e. 0.1, 0.2, 1, 1.5, and 2 $m^{-1}$) modulated by a relative error of −20 or + 20% being representative of the uncertainties associated with the inversion of $a_{cdom}(412)$ from the marine reflectance including those related to atmospheric correction errors [43]. Our results indicate that such uncertainties in $a_{cdom}(412)$ would lead to errors in DOC estimates of 6.2 and −5.4%, respectively, for the $a_{cdom}$-based approach. These relative errors reach 11.4 and −17.9%, respectively, for the $S_{275\text{-}295}$-based approach underlining the cumulative feature of CDOM uncertainties when considering such two steps procedure.

#222294 - $15.00 USD Received 3 Sep 2014; revised 9 Nov 2014; accepted 10 Nov 2014; published 5 Jan 2015

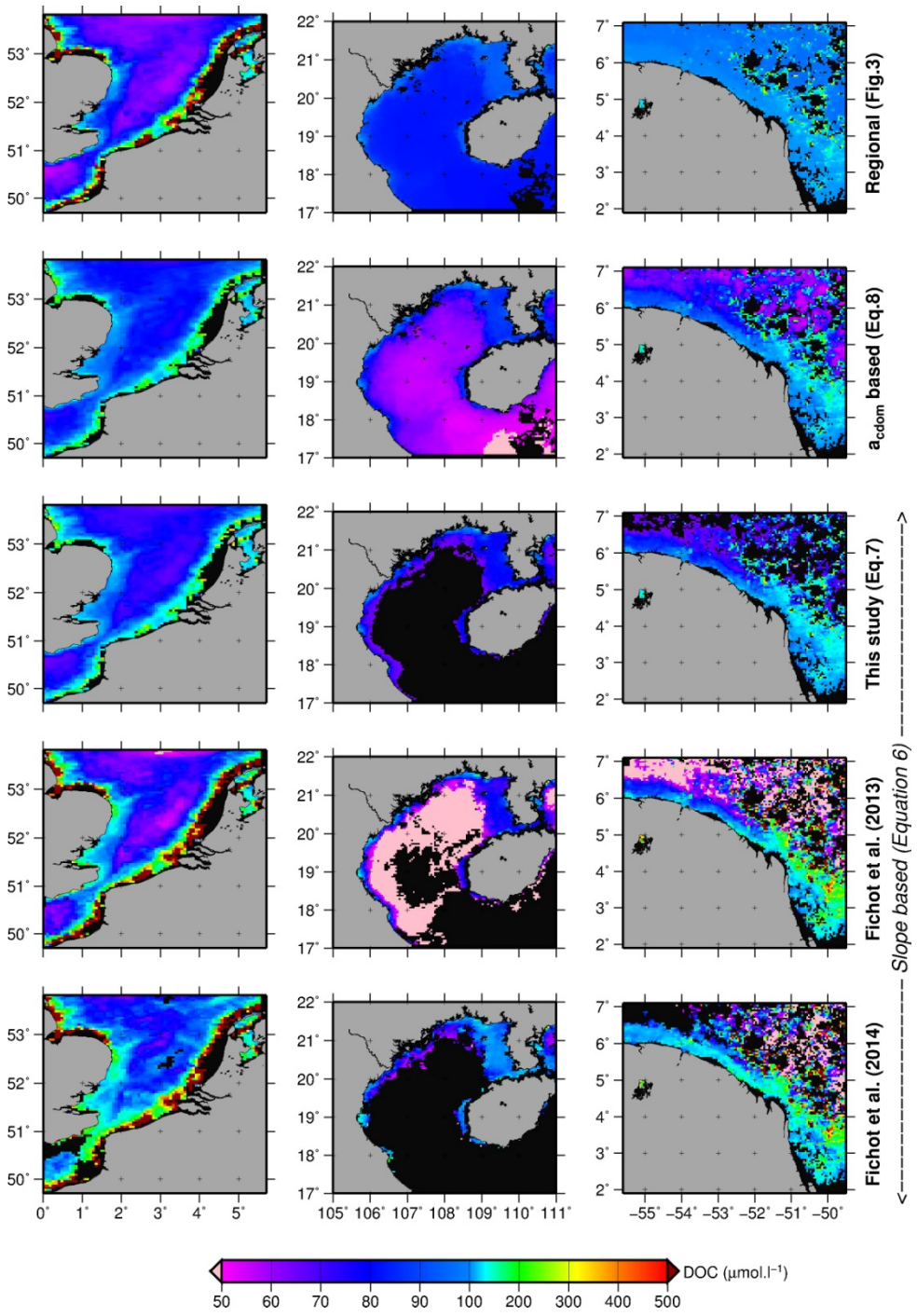


Fig. 11. MODIS DOC distribution in the eastern English Channel, Vietnamese and French Guiana coastal waters estimated from regional relationships (Fig. 3), $a_{cdom}$-based generalized formulation (Eq. (8)) and $S_{275\text{-}295}$ -based relationships (Eq. (6)) with $S_{275\text{-}295}$ estimated from $a_{cdom}(412)$ (Eq. (7)) or from the reflectance according to Fichot et al. [20, 44]. $a_{cdom}(412)$ was computed from the MODIS reflectance using the recent algorithm by Loisel et al. [43]. Black pixels indicate invalid reflectance data or data out of the limits of applicability of the different approaches proposed (see text).

#222294 - $15.00 USD Received 3 Sep 2014; revised 9 Nov 2014; accepted 10 Nov 2014; published 5 Jan 2015

An illustration of the potential limitations associated with the different possible methods for deriving DOC from ocean color remote sensing is presented in Fig. 11 for an application on MODIS monthly data. In practice, $a_{cdom}(412)$ was estimated from the recent algorithm proposed by Loisel et al. [43] based on the semi-analytical relationships between $a_{cdom}(412)$ and $K_d$ at different wavelengths. DOC content were then computed considering individual regional $a_{cdom}$-DOC relationships (Fig. 3), $a_{cdom}$-based (Fig. 7, Eq. (8)), and $S_{275\text{-}295}$-based approaches (Eq. (6), Fig. 4). For the latter two steps procedure $S_{275\text{-}295}$ was computed from $a_{cdom}(412)$ following the parameterization in Eq. (7) (Fig. 6) or from the MODIS reflectance signal according to Fichot et al. [20] and [44].

Globally, limitations in the applicability of linear regional $a_{cdom}(412)$-DOC parameterizations are clearly visible from the persistence of high DOC content especially in the coastal waters of French Guiana and Vietnam (Fig. 11). This lack of spatial dynamics illustrates that simple linear regression between CDOM and DOC are only usable on a very restricted DOC range being unable to fully capture the natural variation of these parameters further underlining the interest of deriving unified approaches.

While the generalized approaches proposed in this study are designed to be representative of a larger range of CDOM and DOC variability they also demonstrate some specific limitations. Algorithms using $S_{275\text{-}295}$ as an intermediary step for deriving DOC are limited, through the formalism in Eq. (6), to water masses showing $S_{275\text{-}295} > 0.03$ $nm^{-1}$ which roughly corresponds to $a_{cdom}(412) < 0.07$ $m^{-1}$, mostly corresponding to offshore waters of Vietnam. This feature can be related to the narrow $S_{275\text{-}295}$ range used in the frame this study ($S_{275\text{-}295}<$ 0.025 $nm^{-1}$) for deriving unified $S_{275\text{-}295}$-$a^*_{cdom}(412)$ parameterization and emphasizes the need to develop such relationships over a wider data set allowing to better represent low DOC conditions [44]. The impact of the input parameters considered for deriving $S_{275\text{-}295}$ is for instance particularly remarkable in the shallow waters of the English Channel where the use of reflectance data [20, 44] leads to a strong over-estimation of DOC content when compared to $a_{cdom}(412)$ based algorithms (Eq. (7)). As a matter of fact, absolute relative differences between DOC estimates computed from $S_{275\text{-}295}$ estimated from $a_{cdom}(412)$ or from the marine reflectance [20, 44] can reach up to a factor of 8 (with DOC reaching unrealistic values of up to 3000 $\mu M.l^{-1}$) in the most turbid waters. This further underlines the potential limitation in the applicability of this $R_{rs}$-based approach for deriving large scale $S_{275\text{-}295}$ and DOC in particularly in highly turbid waters where high CDOM loads also often prevail. Further in the latter environments, which are likely to be associated with low $S_{275\text{-}295}$ values (<0.02 $nm^{-1}$), small variation in the estimates of CDOM slope in the UV can lead to large errors in $a^*_{cdom}(412)$ and therefore in DOC (Fig. 4).

Conversely, the direct relationships between of $a_{cdom}(412)$ and $a^*_{cdom}(412)$ in addition to its lower sensitivity to errors in remotely sensed $a_{cdom}(412)$ are not subject to the latter limitations towards extreme DOC values. While a global consistency is found in DOC estimates computed from $a_{cdom}(412)$ or $S_{275\text{-}295}$ based approaches in slightly turbid waters (relative differences ranging from 10 to 20%) the estimation of DOC from $a_{cdom}(412)$-based algorithm generally allows for the greater spatial coverage in DOC for the different sites investigated. For these reasons, this alternative appears to be particularly suitable for deriving large scale estimate of DOC from spatial observation and should be explored through larger investigations.

## 4. Conclusions

This study aimed at characterizing variations in the $a_{cdom}$-DOC relationships in three contrasted coastal sites: the eastern English Channel, the Tonkin Gulf and the French Guiana coastal margin (78% of the data set is directly under the influence of river inputs, the remaining part being more under oceanic influence). Strong regional linear relationships can be drawn between CDOM absorption and DOC loads in each area investigated suggesting the possible estimation of DOC content from CDOM in the latter coastal regions. While the

#222294 - $15.00 USD Received 3 Sep 2014; revised 9 Nov 2014; accepted 10 Nov 2014; published 5 Jan 2015

results obtained in the frame of this study logically confirm the impossible generalization of direct estimates of DOC from $a_{cdom}$, they also clearly demonstrated the restricted applicability of such regional formulations (see Fig. 11).

This study however agrees with the statement by Fichot and Benner [15] demonstrating the potential for $S_{275\text{-}295}$ to be used as a relevant tracer of DOM terrestrial inputs and thus of $a^*_{cdom}(412)$ variability. Our results have further evidenced that knowledge on CDOM spectral signature in the UV can be used to monitor coastal waters regional variations in $a^*_{cdom}(412)$ being therefore of particular interest for deriving large scale estimates of DOC content from $a_{cdom}(412)$ in the latter oceanic domains. The practical use of the information carried by the CDOM UV slope in the context of remote sensing applications appears however to be present various limitations. The significant connection between $S_{275\text{-}295}$ and the marine remote sensing reflectance shows a strong dependence with water optical quality being particularly conditioned by the dominant contribution of CDOM to the water absorption budget as well as to a strong co-variation between dissolved and particulate matter dynamics. Further, the use of a multi-linear combination of marine reflectance signal for deriving $S_{275\text{-}295}$ in the UV appeared to be highly sensitive to the impact of atmospheric corrections errors, leading to a great over-estimation of DOC loads in the most turbid coastal waters thus representing a real issue for spatial application dedicated to coastal environments.

Conversely, this study has demonstrated the possible use of alternative approaches to synoptically derive DOC concentration in coastal margins. Indeed, in the assumption of terrestrial-dominated systems, regional variation in $S_{275\text{-}295}$ and $a^*_{cdom}(412)$ are, to a first order, related to $a_{cdom}(412)$ as thus to the importance of DOM terrestrial inputs. This has been evidenced from a data set gathering together samples from the three coastal sites investigated and further confirmed on an external data set covering a wide range of coastal ecosystems (with DOC ranging from 50 to 250 $\mu mol.L^{-1}$). Among the possible generalized formulations, the development of direct parameterization between $a_{cdom}(412)$ and $a^*_{cdom}(412)$ appears to represent a compelling alternative in the context of remote sensing applications, since it is less sensitive to atmospheric correction errors allowing therefore for a greater spatial coverage than approaches considering $S_{275\text{-}295}$ as an intermediary proxy for estimating DOC concentration from spatial observation.

**Acknowledgments**

The authors would like to thank all participants and voluntary contributors for collecting data that have been assembled in the SeaBass data set. R. Sempéré, B. Charrière and E. Rochelle-Newall are kindly acknowledged for sharing their DOC and CDOM data. This study has been performed in the frame of the GlobCoast (www.foresea.fr/globcoast) which is funded by the Agence Nationale de la Recherche (ANR-11-BLAN-BS56-018-01). The GlobCoast project is affiliated to the LOICZ and AQUIMER project. This work has also been supported by the French Spatial Agency (CNES) through the TOSCA program in the frame of the MODOC and VITEL projects. The authors wish to acknowledge the two anonymous reviewers for their detailed and helpful comments to the manuscript.